scientific reports

Check for updates

OPEN

Investigation on hydrogenation performance of $Mg_{17}Al_{12}$ by adding Y

Hua Ning[1], Guang Wei[1], Jianhong Chen[1], Zhipeng Meng[1]✉, Zhiwen Wang[1], Zhiqiang Lan[2], Xiantun Huang[3], Junyu Chen[4]✉, Peilin Qing[3]✉, Haizhen Liu[2], Wenzheng Zhou[2] & Jin Guo[2]

The mechanism of Y on H/H_2 adsorption performance of $Mg_{17}Al_{12}$ were studied by the density functional theory. We obtained that for the Y-adsorbed systems, Y tended to occupy on the bridge site between adjacent Mg atoms. For the Y-substituted surfaces, Y atoms inclined to replace Mg atoms on the surfaces. We found that hydrogen (H/H_2) absorption on the $Mg_{17}Al_{12}$(110) systems were improved by adding Y, the order of adsorption energy was as follows: clean $Mg_{17}Al_{12}$(110) > the Y-substituted surfaces > the Y-adsorbed surfaces. In addition, H_2 molecules could dissociate on the Y-containing systems without barrier energy. Electronic properties showed that for H_2 adsorption, the s states of atomic H mainly hybridized with the d states of Y. The formations of the Y-H bonds and the interactions between Y and H atoms could expound the mechanism for the promoted hydrogenation performance of the Y-containing surfaces.

Keywords DFT, Mg-based hydrogen storage materials, Adsorption, Dissociation

Magnesium-based hydrogen storage materials have been studied extensively in past twenty years. However, the high dehydrogenation temperature limits their application on mobile energy devices. Researchers have found that adding transition metals (TM) could promote the hydrogen storage of Mg-based materials[1–10]. In details, magnesium was coated by transition metals to form core–shell like structures[1]. The desorption temperatures and dehydrogenation kinetics of these core–shell structures were improved. Moreover, de/hydrogenation properties of MgH_2 with doping 8 mol % TM (TM=Al, Ti, Fe, Ni, Cu and Nb) have been studied by Shang et al.[2]. Their results indicated that the MgH_2 + Ni mixture had the optimal thermodynamic and kinetic performance for dehydrogenation at 300 °C. Lee et al.[9] have found that the hydrogen capacities and kinetic properties of $Mg_{17}Al_{12}$ with adding Ni were increased at 300 °C. Following, the $Mg_{17}Al_{12}$ + TM (TM=Ti, V, and Ni) samples have been synthesized by sintering and ball milling methods[10]. The experimental results reported that the $Mg_{17}Al_{12}$ + V mixture showed the best performances, and desorbed H_2 at 244 °C. Compared with the $Mg_{17}Al_{12,}$ the activation energy of $Mg_{17}Al_{12}$ + V alloy was evidently decreased.

The 4d TM yttrium (Y) belongs to early 4d elements, which are lighter than other 4d transition metals. Moreover, Y belongs to rare earth elements, compared with other rare earth elements (La, Ce, Pr, Nd, and Sm), Y has a smaller atomic mass. The researches on improving the de/hydrogenation performance and hydrogen storage kinetics of magnesium-based hydrogen storage materials using Y as a catalyst have been reported[11–21]. It has been found that Mg-Y-TM (TM=Ni, Cu, Ti, and Fe) ternary or quaternary alloys showed better hydrogen storage performances[22–24]. Such as de/hydrogenation kinetics of magnesium-based materials by adding Y have been studied by Zhang et al.[11]. They indicated that the addition of Y significantly promoted the kinetics performances of the materials. At 380 °C during 12 min, the $Mg_{24}Y_3$ could desorb 5.4 wt.% of hydrogen. Moreover, Pourabdoli et al.[12] have prepared the Ni-Mg-Y samples and reported that dehydrogenation temperatures of MgH_2 were improved with addition of 10 wt.% 9Ni-2Mg-Y alloy. Subsequently, Pourabdoli et al.[13] have studied the effects of Ni-Mg-4Y on dehydrogenation of magnesium hydride. They found that decreased hydrogen

[1]School of Mathematics and Physics, Guangxi Minzu University, Nanning 530006, People's Republic of China. [2]School of Physical Science and Technology, Guangxi University, Nanning 530004, People's Republic of China. [3]Guangxi Key Laboratory of Green Manufacturing for Ecological Aluminum Industry & Engineering Research Center of Advanced Aluminium Matrix Materials of Guangxi Province, Department of Materials Science and Engineering, Baise University, Baise 533000, People's Republic of China. [4]Guangxi Key Laboratory of Advanced Structural Materlals and Carbon Neutallzation, School of Materials and Environment, Guangxi Minzu University, Nanning 530100, People's Republic of China. ✉email: nickpeng1314@qq.com; lesfaye@163.com; plqing110@163.com

desorption temperatures of magnesium hydride were obtained by adding 10 wt.% Ni-Mg-4Y. Recently, hydrogenation of magnesium/magnesium hydride adding by 5Ni-TM (TM=Ce, Nd, Pr, Sm, and Y) alloys have been investigated[14]. It was reported that formed Mg_2Ni and YH_2 played the role of an effective catalyst. Yong et al.[15] have investigated the hydrogenation of $Mg_{90}Y_{1.5}Ce_{1.5}Ni_7$ mixture and obtained that the mixture had excellent reversible cycle performance and lower hydrogen adsorption temperature (200 °C). It is reported that Y_2O_3 is an effective catalyst for improving the hydrogen storage performance of Mg. The decreased stability of MgH_2 and hydrogenation enthalpy of the Mg-Y_2O_3 composite were obtained[16]. In addition, Lan et al.[17] have synthesized the Y_2O_3-decorated graphene nanocomposite via impregnation processing, and reported that de/hydrogenation temperatures of Mg–Al alloy reduced after adding Y_2O_3-decorated graphene. Following, the hydrogen storage performances of magnesium hydride with doping YH_2 and Co-decorated C catalyst have been investigated[18].

In theory, catalytic effect of Al and Y co-doped MgH_2 was studied by density functional theory (DFT)[25]. In the co-doped case, the hydrogen dissociation energy and dehydrogenation enthalpy were decreased due to strong interaction of Y with Mg and Al. Following, the role of Ni and Y atoms on de/hydrogenation of magnesium hydride was calculated[26]. Their results showed that the hybridization between TM and Mg (H) atoms could obviously weaken interactions of Mg-H bonds.

The above experimental and theoretical results show that the Y and compounds/complexes containing Y doped Mg-based hydrogen storage materials can reduce the thermodynamic stability and promote the kinetics performance, however, the effect of Y on the hydrogen storage properties of Mg-based alloy remains unknown. As a classical Mg-based hydrogen storage materials, the effect of Y doped $Mg_{17}Al_{12}$ is scarcely reported. In order to comprehend the role of Y doping on hydrogenation of $Mg_{17}Al_{12}$, theoretical investigation of the hydrogen storage performance of Y-doped is very necessary.

In this paper, Y is selected to add in Mg–Al alloy to improve the hydrogen storage performance. For the sake of study on the positive effect of Y, the role of Y on hydrogenation of $Mg_{17}Al_{12}$ are investigated. The hydrogen adsorption and dissociation properties on the $Mg_{17}Al_{12}$(110) surface with addition of Y are calculated in detail. Moreover, their interrelated electron densities, projected density of states (PDOS), and electron density difference are discussed.

Calculation model and method

In this paper, the space group structure of $Mg_{17}Al_{12}$ was $I\bar{4}3\,m$, lattice parameter was a = 10.55Å, α = β = γ = 90°. The model of bulk M $g_{17}Al_{12}$ contained 34 magnesium and 24 aluminum atoms, which was plotted in Fig. 1a. The magnesium atoms in the bulk model occupied at three different positions, which were 2a, 8c, and 24g, labeling Mg_1, Mg_2, and Mg_3, respectively, and the aluminum atom occupied at 24g position[27]. X-ray diffraction results of $Mg_{17}Al_{12}$ alloy displayed that the (660), (550) and (330) surfaces showed significant diffraction peaks, and the peaks with high index numbers had strong diffraction intensity[28,29]. Thus, the (110) surface was used to explore the hydrogenation process of $Mg_{17}Al_{12}$ alloy comprehensively. For $Mg_{17}Al_{12}$(110) surfaces, the structure contained 17 magnesium and 12 aluminum atoms. Three layers for the $Mg_{17}Al_{12}$(110) surface were defined (shown in Fig. 1b). We fixed atoms at the 2nd and 3rd layers, and the rest of atoms were released. For Y-substituted systems, the three labeled Mg (Mg1, Mg2, and Mg3) and Al (Al_{surf}, Al_{sub1}, and Al_{sub2} on surface) atoms in the bulk $Mg_{17}Al_{12}$ and the (110) surfaces were substituted by one (or two) Y atoms, and the corresponding structures were named $Mg_{33}YAl_{24}$, $Mg_{34}Al_{23}Y$, $Mg_{16}YAl_{12}$(110), $Mg_{15}Y_2Al_{12}$(110), and $Mg_{17}Al_{11}Y$(110), respectively. The related cohesive energy (E_{coh})[30] of the $Mg_{17}Al_{12}$ with doping Y, as well as the formation energy (E_{for}) and adsorption energy (E_{ads}) of the $Mg_{17}Al_{12}$(110) with adding Y surfaces were defined as following formulas.

$$E_{coh}\left(Mg_{33}YAl_{24}\right)=E_{tot}-33E_{Mg}-24E_{Al}-E_Y$$

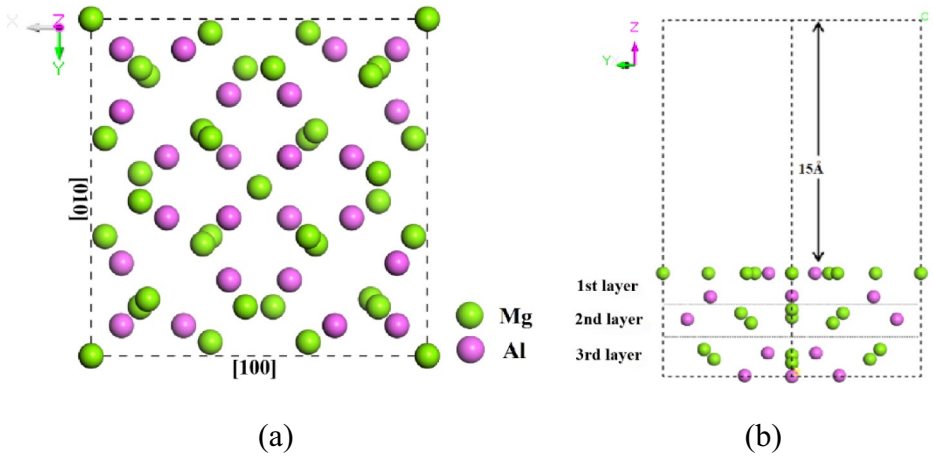

Figure 1. (**a**) The structures of bulk $Mg_{17}Al_{12}$ and (**b**) the $Mg_{17}Al_{12}$(110) surface (side view).

$$E_{coh}\left(Mg_{34}Al_{23}Y\right)=E_{tot}-34E_{Mg}-23E_{Al}-E_{Y}$$

$$E_{for}=\frac{1}{29}\left(E_{tot}\text{-}12E_{Al}-(17\text{-}b)E_{Mg}\text{-}bE_{Y}\right)$$

$$E_{ads}=E_{surface/adsorbate}-E_{surface}-E_{adsorbate}$$

where the E_{tot} represented the total energies of the Y-containing structures, E_{Mg}, E_{Al}, and E_Y denoted the total energies of the single atom, respectively. The $E_{surface/adsorbate}$ and $E_{surface}$ represented the total energies of systems with adsorbates and clean systems, respectively. The $E_{adsorbate}$ represented the total energies of Y or H (H_2).

In our calculation, geometry and electronic structures of the $Mg_{17}Al_{12}(110)$ surfaces with adding Y were calculated with the Cambridge Serial Total Energy Package (CASTEP)[31]. Exchange correlation potential was used the generalized gradient approximation (GGA) with Perdew, Burke, Ernzerhof (PBE)[32]. The $6\times6\times6$ Monkhorst–Pack was used for the $Mg_{17}Al_{12}$ alloy, and the $6\times6\times1$ Monkhorst–Pack was used for $Mg_{17}Al_{12}(110)$ surfaces. 330 eV was chosen for cutoff energy, the residual force was 0.05 eV/Å, the maximum stress was 0.1Gpa, the displacement was 0.002Å, and the maximum energy change was used to 2.0×10^{-5} eV/atom[33]. To include the vander Waals interaction, the DFT-D correction[34] was used. Furthermore, the linear synchronous transit and quadratic synchronous transit calculations were chosen to calculate barrier energies of H_2 dissociation.

Results and discussion

Y-containing $Mg_{17}Al_{12}$ and $Mg_{17}Al_{12}(110)$ surfaces

For alloy, the cohesive energies and lattice constants of $Mg_{17}Al_{12}$ with doping Y are listed in Table 1. We obtain that the cohesive energies of $Mg_{33}YAl_{24}$ are lower than the $Mg_{34}Al_{23}Y$, indicating that Y is easier to replace Mg in the $Mg_{17}Al_{12}$ alloy. The doping of Y increases the volumes of the $Mg_{17}Al_{12}$ alloy. The lattice constants of *a, b,* and *c* for bulk $Mg_{17}Al_{12}$ are all extended by Y substituting for Mg (or Al) on the bulk. The cohesive energies of $Mg_{16}YAl_{12}$ are about − 2.45 eV, which is lower than that of $Mg_{17}Al_{11}Y$ system (− 2.38 eV). Our results show that the lattice parameter, equilibrium volume, and heat of formation energy of bulk $Mg_{17}Al_{12}$ are 10.57 Å, 1173.97 $Å^3$, and − 0.050 eV/atom, respectively, which are in agreement with the experimental results (10.55 Å, 1173.80 $Å^3$ and − 0.048 eV/atom) and other theoretical values[35–38]. Furthermore, the computed surface energy (656 mJ/m^2) of $Mg_{17}Al_{12}(110)$ surface is in line with Ref.[28] (662 mJ/m^2).

In cases of the Y-containing $Mg_{17}Al_{12}$ (110) surfaces, two types of structures are considered, including the Y substitution for Mg (or Al) on the surfaces and Y adsorption on the surfaces. In details, for the Y-substituted surfaces, we use one or two Y atom(s) instead of one Mg (or Al) atom on the surfaces.

For the Y-adsorbed surfaces (labeled by $Mg_{17}Al_{12}(110)/Y$), the adsorption sites, including top sites of the magnesium and aluminum (A, B, C, D, E, and F), and bridge sites between Mg and Mg (Al) (G, H, I, J, K, M, and N), and bridge site between Al and Al (L), are displayed in Fig. 2. In Table 2, the adsorption energies (E_{ads}) of Y adsorption on the $Mg_{17}Al_{12}(110)$ surfaces as well as the formation energies (E_{for}) of the Y-substituted surfaces are presented.

For the Y-adsorbed systems, one Y tends to occupy on the bridge sites of Mg-Mg bonds (such as F and I sites), or the top sites of Al atom (such as E sites), the distance between the Mg and Y atoms are in the range from 2.95 to 3.36 Å. The best adsorption site for Y on the $Mg_{17}Al_{12}(110)$ surfaces is the E site with the minimum adsorption energy. For the Y-substituted systems, the formation energies of the $Mg_{16}YAl_{12}(110)$ surfaces are lower than those of the $Mg_{17}Al_{11}Y(110)$ surfaces, suggesting that one Y atom is easier to replace one Mg atom on the surfaces. The structure of $Mg_{16}YAl_{12}(110)$ (Mg_1) has the lowest formation energy. The models of two Y atoms replacing two Mg atoms on the surfaces are discussed and the substitution atoms are labeled $Mg_{1\text{-}2}$, $Mg_{1\text{-}3}$, $Mg_{2\text{-}3}$, and $Mg_{3\text{-}3}$, respectively. It is seen that compared with the $Mg_{16}YAl_{12}(110)$ systems, the formation energies of $Mg_{15}Y_2Al_{12}(110)$ systems are lower, suggesting that the $Mg_{15}Y_2Al_{12}(110)$ surface is more stable.

One H atom adsorption on the Y-containing surfaces

Atomic hydrogen adsorption on the $Mg_{17}Al_{12}(110)$ systems with Y are studied in this section. The bridge sites of the Mg-Mg and Mg-Y bonds as well as the top sites of Mg and Y are considered for adsorbing H. Initial adsorption height of one H on the surfaces is set to 3.0 Å. The E_{ads} and structural parameters of atomic H adsorption on the surfaces with adding Y are listed in Table 3. Calculations suggest that the E_{ads} of one H absorption on the $Mg_{17}Al_{12}(110)$ systems are improved by adding Y, the order of adsorption energy is

Systems	E_{coh}(eV)	Lattice constant (Å)		
		a	b	c
$Mg_{34}Al_{24}$	− 2.37	10.55	10.55	10.55
$Mg_{33}YAl_{24}(Mg_1)$	− 2.45	10.68	10.68	10.68
$Mg_{33}YAl_{24}(Mg_2)$	− 2.45	10.70	10.70	10.70
$Mg_{33}YAl_{24}(Mg_3)$	− 2.44	10.71	10.71	10.74
$Mg_{34}Al_{23}Y$ (Al)	− 2.38	10.74	10.74	10.80

Table 1. Cohesive energies and lattice constants of the Y-substituted $Mg_{17}Al_{12}$.

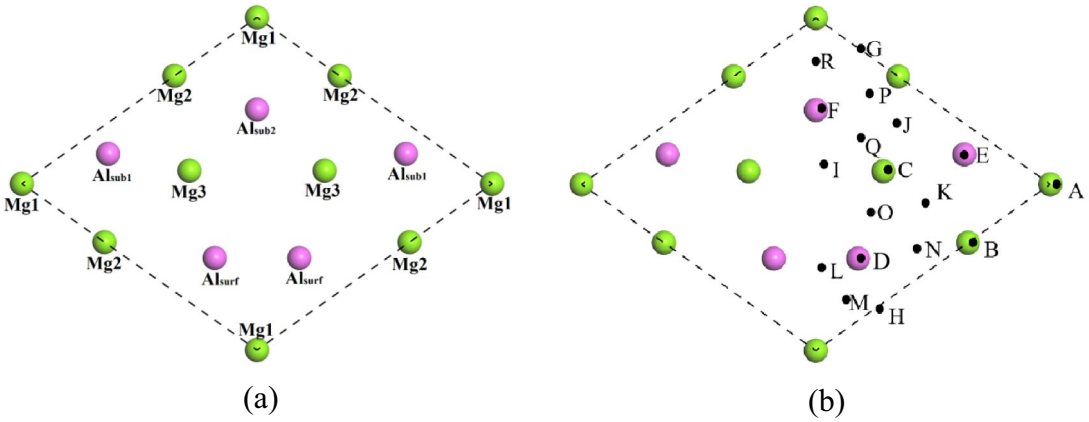

Figure 2. Top views of (**a**) $Mg_{17}Al_{12}(110)$ surfaces in the topmost layer and (**b**) adsorption sites of Y.

Surfaces	Systems	adsorption sites	substitution atoms	$E_{ads/for}$(eV)
clean	$Mg_{17}Al_{12}(110)$[26]	–	–	−2.11
Y-adsorbed	$Mg_{17}Al_{12}(110)/Y$	E	–	−4.01
		F	–	−3.88
		I	–	−3.74
		L	–	−2.97
		M	–	−2.96
		K	–	−2.70
Y-substituted	$Mg_{16}YAl_{12}(110)$	–	Mg_1	−2.23
		–	Mg_2	−2.22
		–	Mg_3	−2.20
	$Mg_{17}Al_{11}Y$ (110)	–	Al_{surf}	−2.11
		–	Al_{sub1}	−2.12
		–	Al_{sub2}	−2.12
	$Mg_{15}Y_2Al_{12}(110)$	–	$Mg_{1\text{-}2}$	−2.35
		–	$Mg_{1\text{-}3}$	−2.35
		–	$Mg_{2\text{-}3}$	−2.32
		–	$Mg_{3\text{-}3}$	−2.31

Table 2. Adsorption energies (E_{ads}) of Y adsorption on the $Mg_{17}Al_{12}(110)$ systems and formation energies (E_{for}) of the Y-substituted $Mg_{17}Al_{12}(110)$ surfaces.

Systems + one H	Adsorption sites	E_{ads} (eV)	$d_{Mg\text{-}Mg}$ (Å)	$d_{Mg\text{-}Al}$ (Å)	$d_{Mg\text{-}Y}$ (Å)	$d_{Al\text{-}Y}$ (Å)	$d_{Mg\text{-}H}$ (Å)	$d_{Y\text{-}H}$ (Å)	$d_{Al\text{-}H}$ (Å)	$d_{H\text{-}surface}$ (Å)
$Mg_{17}Al_{12}(110)$[41]	J	−0.18	3.13	3.03	–	–	1.91	–	3.43	1.10
$Mg_{17}Al_{12}/Y(110)$	E	−1.21	2.97	3.07	3.21	2.96	1.99	2.18	3.38	1.38
$Mg_{16}YAl_{12}(110)$	G	−0.27	3.12	3.20	3.29	3.19	1.89	2.18	3.51	1.15
$Mg_{15}Y_2Al_{12}(110)(Mg_{1\text{-}2})$	G	−0.76	3.34	3.19	3.40	3.20	4.50	2.18	3.52	1.34
$Mg_{15}Y_2Al_{12}(110)(Mg_{2\text{-}3})$	J	−0.90	3.04	3.04	3.88	3.20	4.83	2.19	3.64	1.32
$Mg_{15}Y_2Al_{12}(110)(Mg_{3\text{-}3})$	I	−0.75	3.46	3.21	3.21	3.14	4.31	2.21	3.37	1.25

Table 3. Adsorption energy(E_{ads}) and the distances between different atoms on the various surfaces with H.

$Mg_{17}Al_{12}(110) > Mg_{16}YAl_{12}(110) > Mg_{15}Y_2Al_{12}(110) > Mg_{17}Al_{12}/Y(110)$. In details, compared with the clean surface, the $Mg_{17}Al_{12}/Y(110)$ system with -1.21 eV adsorption energy is the optimal surface to capture H atoms. In the $Mg_{17}Al_{12}/Y$ (110) surface, atomic H occupies on the bridge site of the Mg-Y bond, the length of the Mg-H bond ($d_{Mg\text{-}H}$) is 1.99 Å, suggesting the formation of Mg-H. That is because the lengths of Mg-H bonds for bulk MgH_2 was 1.94 Å[39]. Next the second preferable surfaces are the $Mg_{15}Y_2Al_{12}(110)$ systems. In the $Mg_{15}Y_2Al_{12}(110)$ surfaces, atomic H adsorbs on the bridge site of the Y-Y bond, the distances between Y and H atoms ($d_{Y\text{-}H}$) are

from 2.18 to 2.21 Å, which is in agreement with those in YH_2 (2.24 Å)[40]. It is noted that the $Mg_{15}Y_2Al_{12}$(110) (Mg_{2}-$_3$) surfaces (− 0.90 eV) have lower adsorption energies than $Mg_{16}YAl_{12}$(110) surfaces (− 0.27 eV).

Following, the electronic structures of atomic H on the $Mg_{17}Al_{12}$(110) surfaces with doping Y are calculated. Figure 3 shows the electron densities of the various $Mg_{17}Al_{12}$(110) surfaces with H. It is seen that H likes to occupy on the bridge sites of the Mg-Y bonds in the $Mg_{17}Al_{12}$/Y(110) and $Mg_{16}YAl_{12}$(110) systems, the interaction of the H and Mg atoms is stronger than that between Y and H. It can be seen in Fig. 3 (a) and (b), the overlap charge density between Mg and H atoms are more obvious than that between Y and H, indicating the stronger interaction between H and Mg atoms.

Next, Fig. 4 displays the related projected density of states (PDOS) and electron density differences of atomic hydrogen adsorption on various systems. For $Mg_{17}Al_{12}$(110)/Y with H systems, the *s* states of Mg atom hybridize with the *s* states of H atom at -6.5 eV below the Fermi level. The related electron density differences show that a large amount of charge accumulate (deplete) around the H (Mg) atom, indicating that the H receives charge from Mg. For H on the $Mg_{16}YAl_{12}$ (110) surface, the peak of hybridization between the Mg s states and H s states is observed in at -6.0 to -3.0 eV below the Fermi level. The H atom accepts most of charge from the surface Mg. In the $Mg_{15}Y_2Al_{12}$(110) system, Fig. 4c illustrates that the Y *d* states hybridize primarily with the H *s* states at -3.5 eV below the Fermi level. The results of PDOS and electron density differences indicate that H receives parts of charge from the Y, the distance between Y and H is 2.19 Å, the Y-H bonds are formed.

Furthermore, the Mulliken population analysis of atomic H on the various surfaces is displayed in Table 4. It is gained that atomic H obtain 0.36–0.44 e after adsorption on the surfaces with Y. In the $Mg_{17}Al_{12}$/Y(110) and $Mg_{16}YAl_{12}$(110) systems, a large amount of charge on the H atoms comes from the Mg and Y, while on the $Mg_{15}Y_2Al_{12}$.

surfaces, the H atoms receive most of charge from Y, these results are consistent with the results of the electron density differences. Such as in case of the H on the $Mg_{17}Al_{12}$/Y(110) surface, the Mg (Y) transfers 0.24 (0.12) e to H, and the H gains 0.38 e from Y in the $Mg_{15}Y_2Al_{12}$(110)(Mg_{2}-$_3$) surface.

H_2 molecules adsorption on the Y-containing systems

Based on results of the H adsorption, H_2 adsorption on the $Mg_{17}Al_{12}$/Y(110), $Mg_{16}YAl_{12}$(110), and $Mg_{15}Y_2Al_{12}$(110) systems are discussed.

The computational models of one vertical and parallel H_2 molecule on the bridge sites of Mg-Y and Y-Y bonds are considered. The E_{ads} and structures of one hydrogen molecule on various systems with Y are presented in Table 5. Calculations show that the adsorption energy of one hydrogen molecule on the $Mg_{17}Al_{12}$(110)/Y system is − 0.79 eV. H_2 molecules tend to adsorb around Y atoms in the various systems. It is found that the H–H bond lengths are elongated in our calculations. Such as, for the H_2 adsorption on $Mg_{17}Al_{12}$/Y(110), $Mg_{16}YAl_{12}$(110), and $Mg_{15}Y_2Al_{12}$(110)(Mg_{3}-$_3$), the H–H bonds are increased from 0.75 to 0.78 Å.

In addition, more than one H_2 molecule (nH_2 (n = 2, 3, 4)) adsorption on the surfaces with adding Y are investigated and displayed in Fig. 5. Table 6 shows adsorption energies and structural parameters of nH_2 (n = 1–4) on the Y-containing $Mg_{17}Al_{12}$ (110) surfaces. With increasing the numbers of hydrogen molecules, the adsorption energies of nH_2 on the various systems are gradually decreasing. Hydrogen molecules are easy to locate on the Y-adsorbed systems than on the Y-substituted systems. In details, there is − 0.51 eV adsorption energy of $4H_2$ on the Y-adsorbed surface, however the adsorption energy of $4H_2$ on the $Mg_{16}YAl_{12}$(110) ($Mg_{15}Y_2Al_{12}$(110)) system is only − 0.04 (− 0.16) eV. The Y-adsorbed surface has strong $4H_2$ adsorption capacity, while $4H_2$ adsorbed on the Y-substituted surface are almost saturation.

Following, the PDOS of one hydrogen molecule on the various systems are showed in Fig. 6. We find that in the different systems, Y *d* states mainly hybrid with H *s* states at − 10.0 to − 8.5 eV, suggesting the strong interaction between Y and H. Furthermore, Table 7 shows the Mulliken population analysis of the various systems with one hydrogen molecule. It is gained that H atoms receive 0.13–0.17e from Y atoms, indicating their strong interaction, which are consistent with the results of the PDOS.

Finally, the dissociation process of one hydrogen molecule on the systems with adding Y are computed and drawn in Fig. 7. Here, for the initial states (IS), the geometries of a H_2 adsorption on the Y-containing surfaces with the lowest adsorption energies are considered. The models of two H on the various surfaces are chosen for the final states (FS). The calculations suggest that there is 0.87 eV dissociation energy for one H_2 on the $Mg_{17}Al_{12}$ (110) system, while one H_2 can dissociate automatically on the Y-containing systems without any barrier energy.

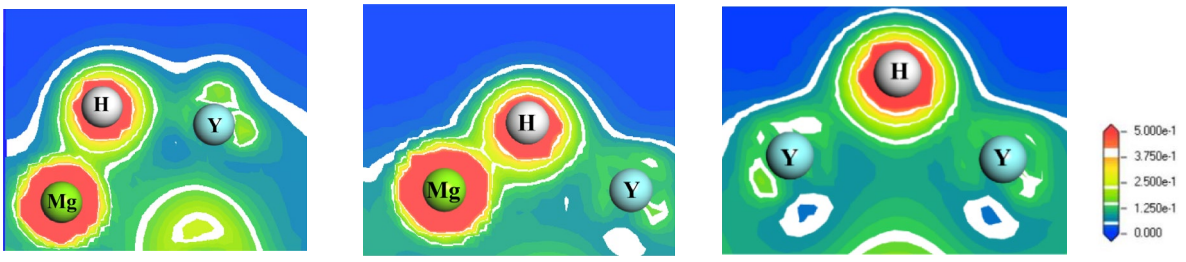

(a) $Mg_{17}Al_{12}$/Y(110) (b) $Mg_{16}YAl_{12}$(110) (c) $Mg_{15}Y_2Al_{12}$(110) (Mg_{2}-$_3$)

Figure 3. Electron densities of hydrogen on the $Mg_{17}Al_{12}$(110) surface with adding Y.

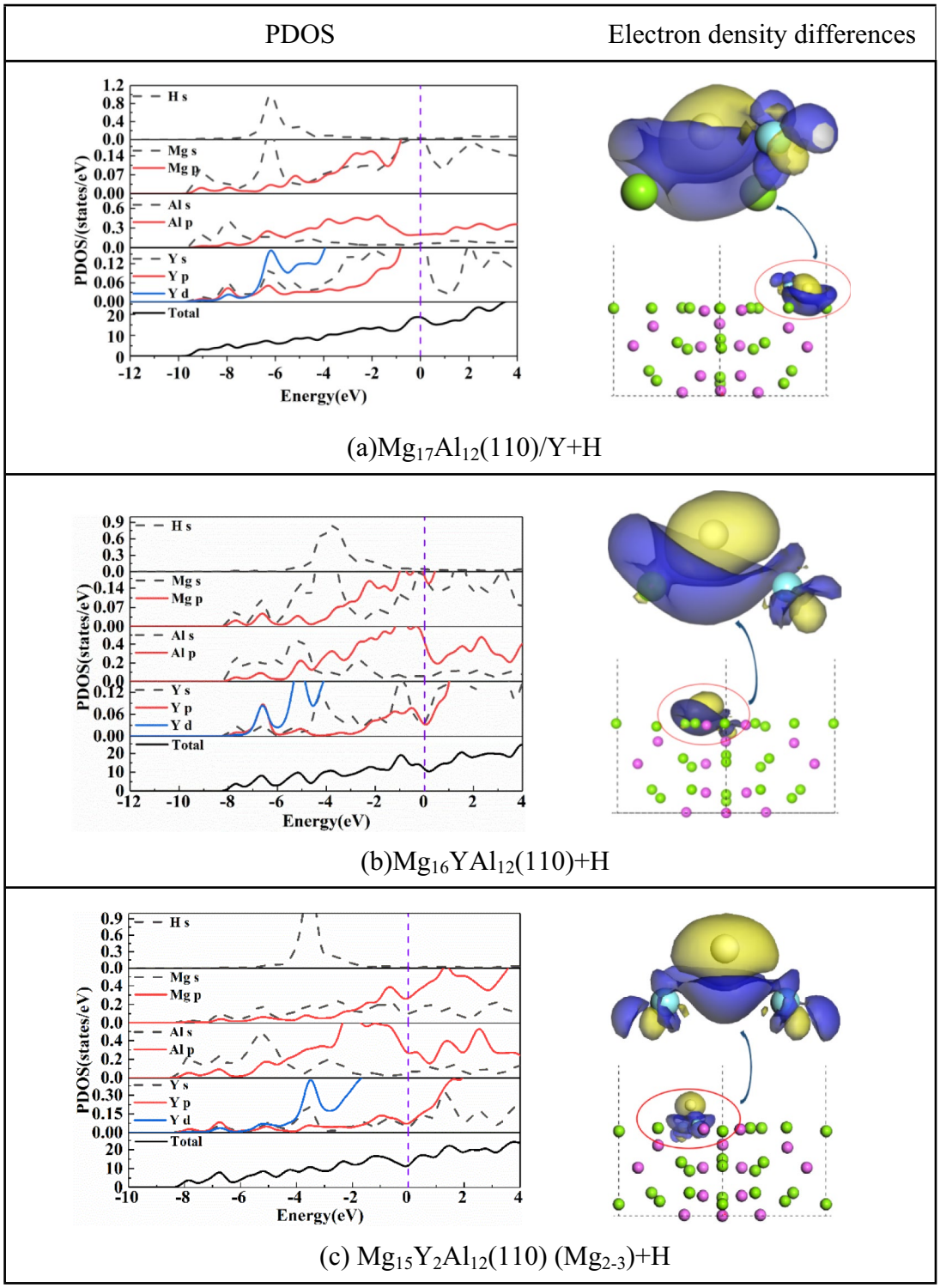

Figure 4. The PDOS and electron density difference of one H adsorption on the $Mg_{17}Al_{12}(110)$ systems with Y (with 0.01 e/Å^3 isosurface value.

The addition of Y evidently assists hydrogen molecule dissociation. In the final states, the distances between two H atoms are elongated from about 0.78 Å to 3.31, 4.08, and 2.57 Å in $Mg_{16}YAl_{12}(110)$, $Mg_{15}Y_2Al_{12}(110)$, $Mg_{17}Al_{12}(110)$/Y systems, respectively, indicating that the H–H bonds are completely broken. Furthermore, the H atoms prefer to adsorb around Y, the distances between Y and H are from 2.14 to 2.21 Å, forming Y-H bonds.

Compared with other similar materials, for TM-adsorbed systems, we find that the $Mg_{17}Al_{12}(110)$/Y system has better hydrogen adsorption and dissociation performances than $Mg_{17}Al_{12}(110)$/(Ti, Ni, V, or Li) systems. For example, the adsorption energy of single H atom on the $Mg_{17}Al_{12}(110)$/Y surface is − 1.21 eV, which is lower

Systems	Surface			Surface + one hydrogen atom			
	Mg	Y	Al	Mg	Y	Al	H
$Mg_{17}Al_{12}$/Y(110)	0.53	− 0.06	− 0.46	0.77	0.06	− 0.49	− 0.43
$Mg_{16}YAl_{12}$(110)	0.31	0.27	− 0.57	0.59	0.54	− 0.56	− 0.44
$Mg_{15}Y_2Al_{12}$(110)(Mg_{1}-$_2$)	0.40	0.20	− 0.49	0.39	0.54	− 0.53	− 0.37
$Mg_{15}Y_2Al_{12}$(110)(Mg_{2}-$_3$)	0.27	0.07	− 0.51	0.25	0.36	− 0.56	− 0.38
$Mg_{15}Y_2Al_{12}$(110)(Mg_{3}-$_3$)	0.32	0.03	− 0.49	0.33	0.26	− 0.50	− 0.36

Table 4. The Mulliken population analysis of a hydrogen atom adsorption on the $Mg_{17}Al_{12}$(110) systems with adding Y.

System + one H_2	E_{ads} (eV)	$d_{Mg\text{-}Mg}$ (Å)	$d_{Mg\text{-}Al}$(Å)	$d_{Mg\text{-}Y}$(Å)	$d_{Al\text{-}Y}$ (Å)	$d_{Mg\text{-}H}$ (Å)	$d_{Al\text{-}H}$ (Å)	$d_{Y\text{-}H}$ (Å)	$d_{H\text{-}H}$ (Å)	$d_{H2\text{-}surface}$ (Å)
$Mg_{17}Al_{12}$(110)	− 0.13	–	2.96	–	–	3.19	–	–	0.76	2.97
$Mg_{17}Al_{12}$(110)/Y	− 0.79	2.93	3.07	3.27	2.94	3.21	4.79	2.51	0.78	1.74
$Mg_{16}YAl_{12}$(110)	− 0.17	3.01	3.01	3.35	3.19	3.84	4.61	2.57	0.78	2.20
$Mg_{15}Y_2Al_{12}$(110)(Mg_{1}-$_2$)	− 0.19	3.43	3.12	3.15	3.20	4.22	3.55	2.55	0.80	1.75
$Mg_{15}Y_2Al_{12}$(110)(Mg_{2}-$_3$)	− 0.18	3.44	3.03	3.49	3.15	4.51	3.73	2.50	0.82	1.70
$Mg_{15}Y_2Al_{12}$(110)(Mg_{3}-$_3$)	− 0.25	3.27	3.07	3.32	3.18	3.68	3.78	2.45	0.78	2.10

Table 5. Adsorption energy (E_{ads}) and the distances between different atoms on the various surfaces with H_2.

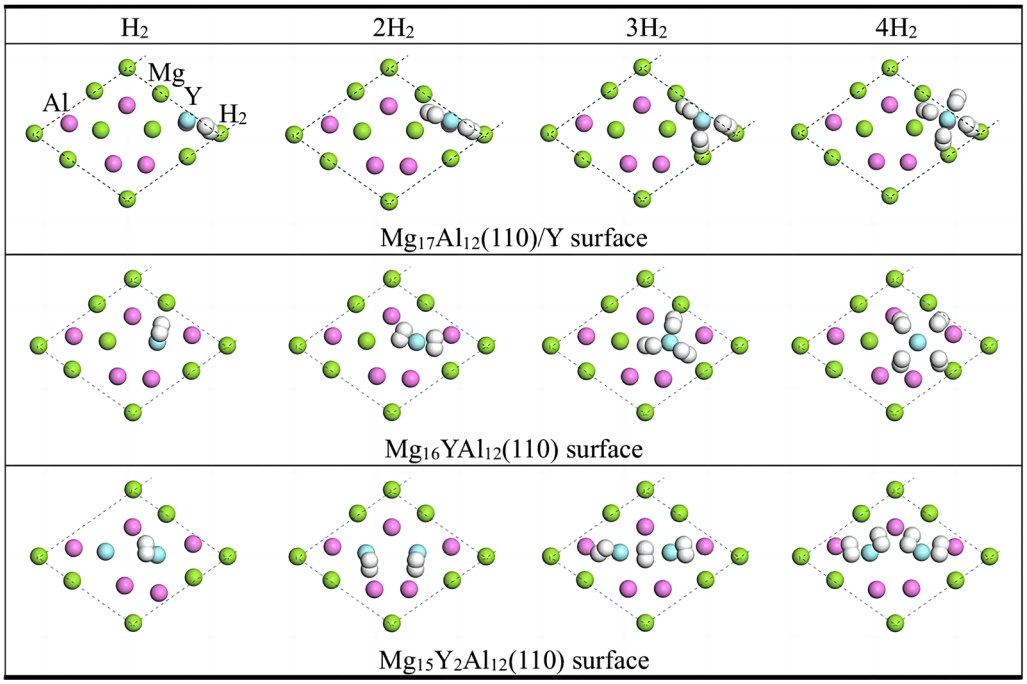

Figure 5. The top views of nH_2(n = 1,2,3,4) adsorption on the $Mg_{17}Al_{12}$ (110) surfaces by adding Y.

than that on the Ti (− 0.70 eV)[42], Li (− 0.68 eV)[43], V (− 0.75 eV)[44], and Ni (− 0.21 eV)[45] adsorbed $Mg_{17}Al_{12}$(110) systems, respectively. Meanwhile, the adsorption energy of H_2 on the $Mg_{17}Al_{12}$(110)/Y surface is -0.79 eV, which is also lower than that on the Ti (− 0.74 eV)[42], V (− 0.73 eV)[44], and Li (− 0.48 eV)[43] adsorbed systems. Furthermore, one H_2 can dissociate on the Y-adsorbed surface without barrier, while the barrier energies of one H_2 dissociation on the Ti, Li, and V adsorbed surfaces are 0.16[42], 0.14[43], and 0.13 eV[44], respectively. Therefore, the Y-adsorbed system is easier to capture H/H_2 and it has better adsorption and dissociation performances than Li, Ti, Ni, and V-adsorbed systems.

Finally, the positive role of Y on hydrogenation of $Mg_{17}Al_{12}$ are comprehended. Compared with other metals (Li, Ti, Ni, and V), the 4d transition metal (Y) is expanded for the catalytic effect on the $Mg_{17}Al_{12}$(110) surface, providing theoretical support for potentially excellent catalysts in experiments.

Systems	nH_2	E_{ads} (eV)	$d_{Mg\text{-}Mg}$ (Å)	$d_{Mg\text{-}Al}$ (Å)	$d_{Mg\text{-}Y}$ (Å)	$d_{Al\text{-}Y}$ (Å)	$d_{Mg\text{-}H}$ (Å)	$d_{Al\text{-}H}$ (Å)	$d_{Y\text{-}H}$ (Å)
$Mg_{17}Al_{12}(110)/Y$	H_2	−0.79	2.93	3.07	3.27	2.94	3.21	4.79	2.51
	$2H_2$	−0.62	2.93	3.06	3.27	2.95	3.27	4.71	2.33
	$3H_2$	−0.56	2.93	3.06	3.26	2.98	2.98	4.58	2.35
	$4H_2$	−0.51	2.93	3.06	3.25	3.01	3.01	4.58	2.34
$Mg_{16}YAl_{12}(110)$ (Mg_3)	H_2	−0.23	3.27	3.13	3.20	314	2.88	4.18	2.47
	$2H_2$	−0.19	3.29	3.13	3.19	3.16	3.56	3.74	2.47
	$3H_2$	−0.06	3.47	3.27	3.15	3.17	2.62	3.90	2.52
	$4H_2$	−0.04	3.47	3.25	3.23	3.18	2.73	4.90	2.45
$Mg_{15}Y_2Al_{12}(110)$ ($Mg_{3\text{-}3}$)	H_2	−0.25	3.27	3.07	3.32	3.18	3.68	378	2.45
	$2H_2$	−0.20	3.27	3.60	3.20	3.12	4.61	4.92	2.44
	$3H_2$	−0.17	3.29	3.59	3.18	3.14	3.37	4.00	2.44
	$4H_2$	−0.16	3.29	3.62	3.15	3.10	3.30	3.60	2.48

Table 6. Adsorption energy (E_{ads}) and the distances between different atoms on the various surfaces with nH_2 (n = 1–4) molecules.

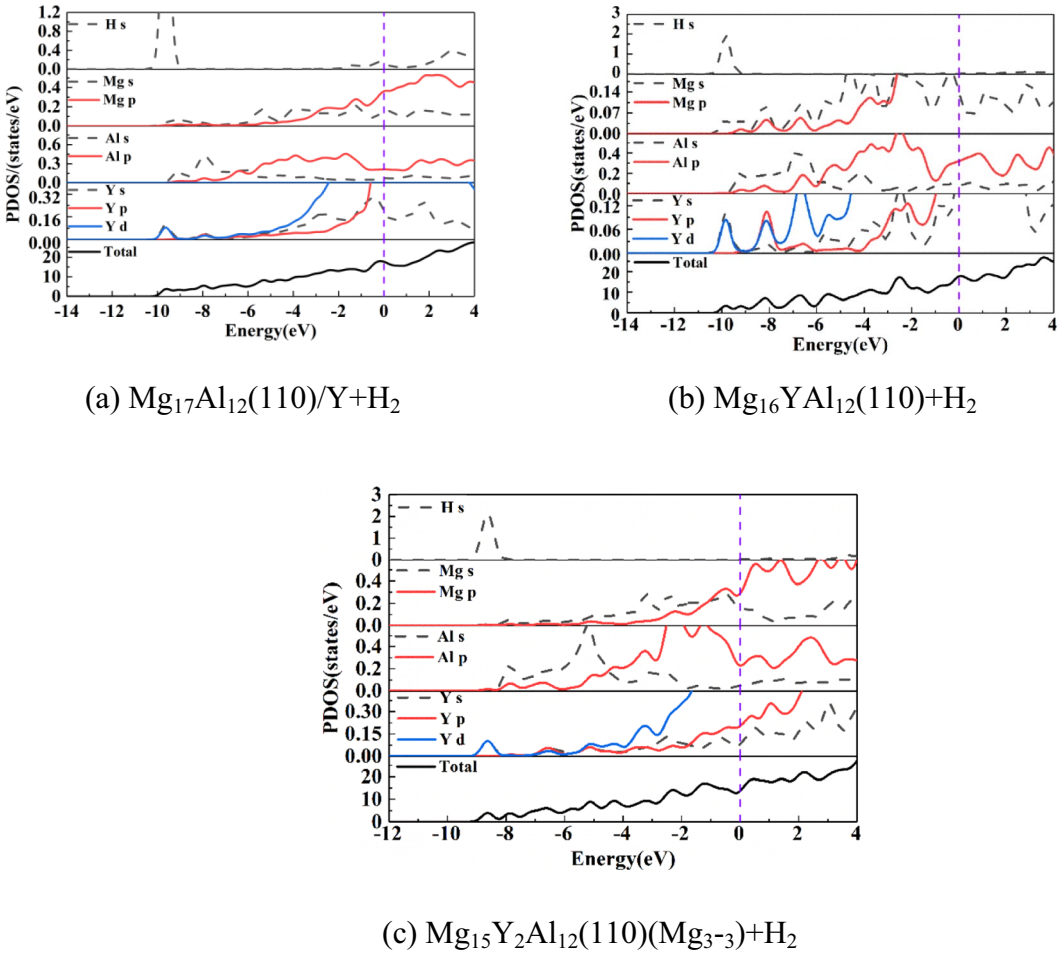

Figure 6. PDOS of one hydrogen molecule on the systems by adding Y.

Conclusion

Based on density functional theory, hydrogenation of $Mg_{17}Al_{12}(110)$ surfaces by adding Y was investigated. Calculations suggested that addition of Y promoted the hydrogenation of the $Mg_{17}Al_{12}(110)$ systems. The order of adsorption energy from high to low was as follows: $Mg_{17}Al_{12}(110) > Mg_{16}YAl_{12}(110) > Mg_{15}Y_2Al_{12}(110) > Mg_{17}Al_{12}/Y(110)$. For multiple hydrogen molecules adsorption systems, there was − 0.51 eV adsorption energy for $4H_2$ molecules on the Y-adsorbed system, more than $4H_2$ could adsorb on the surface, while the Y-substituted surfaces adsorbed

Systems	Surface			Surface + one hydrogen molecule			
	Mg	Y	Al	Mg	Y	Al	H
$Mg_{17}Al_{12}$/Y(110)	0.53	− 0.06	− 0.46	0.53	0.22	− 0.45	− 0.13
$Mg_{16}YAl_{12}$(110)	0.31	0.27	− 0.57	0.31	0.54	− 0.57	− 0.16
$Mg_{15}Y_2Al_{12}$(110) (Mg_{1}-$_{2}$)	0.40	0.1.99	− 0.49	0.41	0.39	− 0.49	− 0.17
$Mg_{15}Y_2Al_{12}$(110) (Mg_{3}-$_{3}$)	0.32	0.03	− 0.49	0.32	0.24	− 0.49	− 0.14

Table 7. The Mulliken population analysis of one hydrogen molecule adsorption on various systems.

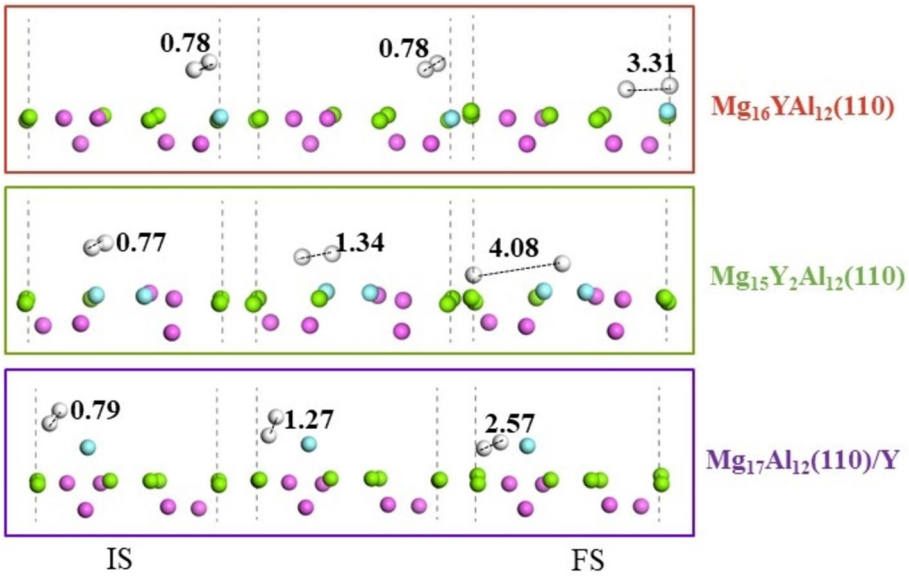

Figure 7. Dissociation process of one hydrogen molecule on the systems with adding Y.

$4H_2$ were almost saturated. Our results obtained that H_2 spontaneously dissociated on the Y-containing surfaces without barrier energy. Compared with other similar metal (Li, Ti, Ni, and V) -adored systems, the Y-adsorbed system had the better adsorption and dissociation performance. Furthermore, the electronic structure calculations revealed that for a H atom adsorption on the $Mg_{17}Al_{12}$/Y(110) and $Mg_{16}YAl_{12}$(110) systems, the interactions between *s* states of Mg and H atoms were obviously below the Fermi level, while for H_2 molecules adsorption, the hybridization between *d* states of Y and *s* states of H atom was strong in various surfaces.

Data availability

The data that support the findings of this study are available on request from the corresponding author. The data are not publicly available due to privacy or ethical restrictions.

Received: 7 June 2024; Accepted: 1 August 2024
Published online: 05 August 2024

References

1. Cui, J. *et al.* Mg-TM (TM: Ti, Nb, V Co, Mo or Ni) core-shell like nanostructures: synthesis, hydrogen storage performance and catalytic mechanism. *J. Mater. Chem. A* **2**, 9645–9655 (2014).
2. Shang, C. X., Bououdina, M., Song, Y. & Guo, Z. X. Mechanical alloying and electronic simulations of (MgH_2+M) systems (M=Al, Ti, Fe, Ni, Cu and Nb) for hydrogen storage. *Int. J. Hydrogen Energy* **29**, 73–80 (2004).
3. Yang, W. N., Shang, C. X. & Guo, Z. X. Site density effect of Ni particles on hydrogen desorption of MgH_2. *Int. J. Hydrogen Energy* **35**, 4534–4542 (2010).
4. Zhang, L. *et al.* Facile synthesized Fe nanosheets as superior active catalyst for hydrogen storage in MgH_2. *Int. J. Hydrogen Energy* **44**, 21955–21964 (2019).
5. Jin, S. A., Shim, J. H., Ahn, J. P., Cho, Y. W. & Yi, K. W. Improvement in hydrogen sorption kinetics of MgH_2 with Nb hydride catalyst. *Acta Mater.* **55**, 5073–5079 (2007).
6. Wang, P. *et al.* Improved hydrogen storage properties of MgH_2 using transition metal sulfides as catalyst. *Int. J. Hydrogen Energy* **46**, 27107–27118 (2021).
7. Shahi, R. R., Tiwari, A. P., Shaz, M. A. & Srivastava, O. N. Studies on de/rehydrogenation characteristics of nanocrystalline MgH_2 co-catalyzed with Ti, Fe and Ni. *Int. J. Hydrogen Energy* **38**, 2778–2784 (2013).
8. Lu, H. B. *et al.* Dehydrogenation characteristics of Ti- and Ni/Ti-catalyzed Mg hydrides. *J. Alloy. Compd.* **481**, 152–155 (2009).
9. Lee, S. *et al.* Effects of Ni addition on hydrogen storage properties of $Mg_{17}Al_{12}$ alloy. *Mater. Chem. Phys.* **126**, 319–324 (2011).

10. Wang, Y. *et al.* Effect of transition metal on the hydrogen storage properties of Mg-Al alloy. *J. Mater. Sci.* **52**, 2392–2399 (2017).
11. Yang, T. *et al.* Improved hydrogen absorption and desorption kinetics of magnesium-based alloy via addition of yttrium. *J. Power Sources* **378**, 636–645 (2018).
12. Pourabdoli, M., Raygan, S., Abdizadeh, H. & Uner, D. A comparative study for synthesis methods of nano-structured (9Ni-2Mg-Y) alloy catalysts and effect of the produced alloy on hydrogen desorption properties of MgH_2. *Int. J. Hydrogen Energy* **38**, 16090–16097 (2013).
13. ChitsazKhoyi, L., Raygan, Sh. & Pourabdoli, M. Mechanical milling of Mg, Ni and Y powder mixture and investigating the effects of produced nanostructured $MgNi_4Y$ on hydrogen desorption properties of MgH_2. *Int. J. Hydrogen Energy* **38**, 6687–6693 (2013).
14. Liao, W. *et al.* Enhancing (de)hydrogenation kinetics properties of the Mg/MgH_2 system by adding ANi_5 (A = Ce, Nd, Pr, Sm, and Y) alloys via ball milling. *J. Rare Earths* **39**, 1010–1016 (2021).
15. Yong, H. *et al.* Characterization of microstructure, hydrogen storage kinetics and thermodynamics of ball-milled $Mg_{90}Y_{1.5}Ce_{1.5}Ni_7$ alloy. *Int. J. Hydrogen Energy* **46**, 17802–17813 (2021).
16. Long, S., Zou, J., Chen, X., Zeng, X. & Ding, W. A comparison study of Mg-Y_2O_3 and Mg-Y hydrogen storage composite powders prepared through arc plasma method. *J. Alloys Compd.* **615**, S684–S688 (2014).
17. Lan, Z. Q. *et al.* Catalytic action of Y_2O_3@graphene nanocomposite on the hydrogen-storage property of Mg-Al alloy. *J. Mater. Chem. A* **29**, 15200–15207 (2017).
18. Xu, C. *et al.* Improved hydrogen absorption/desorption properties of MgH_2 by Co-catalyzing of YH_2 and Co@C. *ChemistrySelect* **4**, 7709–7714 (2019).
19. Zlotea, C., Sahlberg, M., Moretto, P. & Andersson, Y. Hydrogen sorption properties of a Mg-Y-Ti alloy. *J. Alloys Compd.* **489**, 375–378 (2010).
20. Zlotea, C., Sahlberg, M., Özbilen, S., Moretto, P. & Andersson, Y. Hydrogen desorption studies of the $Mg_{24}Y_5$-H system: Formation of Mg tubes, kinetics and cycling effects. *Acta Materialia* **56**, 2421–2428 (2008).
21. Zlotea, C., Lu, J. & Andersson, Y. Formation of one-dimensional MgH_2 nano-structures by hydrogen induced disproportionation. *J. Alloys Compd.* **426**, 357–362 (2006).
22. Kalinichenka, S., Röntzsch, L., Baehtz, C. & Kieback, B. Hydrogen desorption kinetics of melt-spun and hydrogenated $Mg_{90}Ni_{10}$ and $Mg_{80}Ni_{10}Y_{10}$ using in situ synchrotron, X-ray diffraction and thermogravimetry. *J. Alloys Compd.* **496**, 608–613 (2010).
23. Luo, F. P. *et al.* Enhanced reversible hydrogen storage properties of a Mg–In–Y ternary solid solution. *Int. J. Hydrogen Energy* **38**, 10912–10918 (2013).
24. Kalinichenka, S. *et al.* Microstructure and hydrogen storage properties of melt-spun Mg–Cu–Ni–Y alloys. *Int. J. Hydrogen Energy* **36**, 1592–1600 (2011).
25. Zhou, S. C. *et al.* Ab initio study of effects of Al and Y co-doping on destabilizing of MgH_2. *Int. J. Hydrogen Energy* **39**, 9254–9261 (2014).
26. Sun, G. *et al.* First-principles investigation of the effects of Ni and Y co-doped on destabilized MgH_2. *RSC Adv.* **6**, 23110–23116 (2016).
27. Zhang, M. X. & Kelly, P. M. Edge-to-edge matching and its applications. *Acta Materialia* **53**, 1085–1096 (2005).
28. Xiao, W., Zhang, X., Geng, W. T. & Lu, G. Atomistic study of plastic deformation in Mg-Al alloys. *Mater. Sci. Eng. A* **586**, 245–252 (2013).
29. Crivello, J. C., Nobuki, T. & Kuji, T. Limits of the Mg-Al γ-phase range by ball-milling. *Intermetallics* **15**, 1432–1437 (2007).
30. Xiao, X. B., Zhang, W. B., Yu, W. Y., Wang, N. & Tang, B. Y. Energetics and electronic properties of Mg_7TMH_{16} (TM=Sc, Ti, V, Y, Zr, Nb): An ab initio study. *Phys. B Condens. Matter* **404**, 2234–2240 (2009).
31. Segall, M. D. *et al.* First-principles simulation: Ideas, illustrations and the CASTEP code. *J. Phys. Condens. Matter* **14**, 2717–2744 (2002).
32. Perdew, J. P., Burke, K. & Ernzerhof, M. Generalized gradient approximation made simple. *Phys. Rev. Lett.* **77**, 3865–3868 (1996).
33. Fischer, S. & Karplus, M. Conjugate peak refinement: An algorithm for finding reaction paths and accurate transition states in systems with many degrees of freedom. *Chem. Phys. Lett.* **194**, 252–261 (1992).
34. Grimme, S. Semiempirical GGA-type density functional constructed with a long-range dispersion correction. *J. Computat. Chem.* **27**, 1787–1799 (2006).
35. Zhang, M. X. & Kelly, P. M. Edge-to-edge matching and its applications: Part I. Application to the simple HCP/BCC system. *Acta Materialia* **53**, 1085 (2005).
36. Wang, N., Yu, W. Y., Tang, B. Y., Peng, L. M. & Ding, W. J. Structural and mechanical properties of $Mg_{17}Al_{12}$ and $Mg_{24}Y_5$ from first-principles calculations. *J. Phys. D Appl. Phys.* **41**, 195408 (2008).
37. Huang, Z. W., Zhao, Y. H., Hou, H. & Han, P. D. Electronic structural, elastic properties and thermodynamics of $Mg_{17}Al_{12}$, Mg_2Si and Al_2Y phases from first-principles calculations. *Phys. B Condens. Matter.* **407**, 1075–1081 (2012).
38. Bortz, M., Bertheville, B., Bottger, G. & Yvon, K. Structure of the high pressure phase γ-MgH_2 by neutron powder diffraction. *J. Alloys Compd.* **287**, L4 (1999).
39. Zhang, Z., Zhou, X., Zhang, H., Guo, J. & Ning, H. Hydrogen penetration and diffusion on $Mg_{17}Al_{12}$(110) surface: A density functional theory investigation. *Int. J. Hydrogen Energy* **42**, 26013–26019 (2017).
40. Noritake, T. *et al.* Chemical bonding of hydrogen in MgH_2. *Appl. Phys. Lett.* **81**, 2008–2010 (2002).
41. Dai, J. H., Song, Y. & Yan, R. Influences of alloying elements and oxygen on the stability and elastic properties of $Mg_{17}Al_{12}$. *J. Alloys Compd.* **595**, 142–147 (2014).
42. Ning, H. *et al.* Effects of transition metal Ti and its compounds on hydrogen adsorption performance of $Mg_{17}Al_{12}$. *Int. J. Hydrogen Energy* **47**, 13900–13910 (2022).
43. Zhou, X., Ma, S., Xu, S., Guo, J. & Ning, H. Effects of Li on hydrogen absorption properties of $Mg_{17}Al_{12}$(110) Surface: A density functional theory study. *Int. J. Hydrogen Energy* **43**, 18330–18338 (2018).
44. Ning, H. *et al.* Effects of vanadium, vanadium carbide, and vanadium oxide catalysts on hydrogenation of $Mg_{17}Al_{12}$ (110) surface: A first principles study. *Int. J. Hydrogen Energy* **45**, 28078–28086 (2020).
45. Ning, H., Zhou, X., Zhang, Z., Zhou, W. & Guo, J. Ni catalytic effects for the enhanced hydrogenation properties of $Mg_{17}Al_{12}$ (110) surface. *Appl. Surf. Sci.* **464**, 644–650 (2019).

Acknowledgements

This work was supported by National Natural Science Foundation of China (Grant No. 52261038), the Scientific Research Foundation of Guangxi MinZu University, China (2020KJQD01), and the highperformance computing platform of Guangxi University.

Author contributions

Conceptualization, Hua Ning and Zhipeng Meng; Investigation, Xiantun Huang and Peilin Qing; Data Curation, Guang Wei and Junyu Chen; Writing-Original Draft Preparation, Guang Wei and Jianhong Chen; Writing-Review & Editing, Wenzheng Zhou and Zhiwen Wang; Supervision, Zhiqiang Lan, Haizhen Liu, and Jin Guo.

Competing interests
The authors declare no competing interests.

Additional information
Correspondence and requests for materials should be addressed to Z.M., J.C. or P.Q.

Reprints and permissions information is available at www.nature.com/reprints.

Publisher's note Springer Nature remains neutral with regard to jurisdictional claims in published maps and institutional affiliations.